

- W. Giriat, and L. Sosnowski, *Phys. Status Solidi* **8**, K135 (1965); R. Piotrkowski and S. Porowski, in *Proceedings of the Tenth International Conference on II-VI Semiconducting Compounds, Providence, 1967*, edited by D. G. Thomas (Benjamin, New York, 1967), p. 1090.
- ¹⁷G. Weill and C. Vérié, *Compt. Rend.* **263**, 463 (1966).
- ¹⁸C. Vérié and G. Martinez, *Compt. Rend.* **266**, 720 (1968).
- ¹⁹T. C. Harman, MIT Lincoln Laboratory, Solid State Research Report No. 3, p. 2, 1970 (unpublished).
- ²⁰A. G. Foyt (private communication).
- ²¹C. T. Elliott, Ivars Melngailis, T. C. Harman, and A. G. Foyt, *J. Phys. Chem. Solids* (to be published).
- ²²John Melngailis, J. A. Kafalas, and T. C. Harman, *J. Phys. Chem. Solids Suppl.* **32**, 407 (1971).
- ²³I. L. Spain and S. Segall, *Cryogenics* **11**, 26 (1971).
- ²⁴J. S. Dugdale, in *Advances in High Pressure Research*, edited by R. S. Bradley (Academic, New York, 1969), Vol. 2, p. 105.
- ²⁵W. S. Goree and T. A. Scott, *J. Phys. Chem. Solids* **27**, 835 (1966).
- ²⁶A. C. Beer, *Galvanomagnetic Effects in Semiconductors* (Academic, New York, 1963).
- ²⁷D. J. Howarth, R. H. Jones, and E. H. Putley, *Proc. Phys. Soc. (London)* **70**, 124 (1957).
- ²⁸J. L. Schmit, *J. Appl. Phys.* **41**, 2876 (1970).
- ²⁹T. C. Harman and A. J. Strauss, *J. Appl. Phys.* **32**, 2265 (1960).
- ³⁰M. W. Scott, *J. Appl. Phys.* **40**, 4077 (1969).
- ³¹G. W. Iseler, J. A. Kafalas, and A. J. Strauss, MIT Lincoln Laboratory, Solid State Research Report No. 2, p. 29, 1971 (unpublished).
- ³²D. R. Scifres, N. Holonyak, Jr., C. B. Duke, G. G. Kleiman, A. B. Kunz, M. G. Crawford, W. O. Groves, and A. H. Herzog, *Phys. Rev. Letters* **27**, 191 (1971).
- ³³N. F. Mott, *Rev. Mod. Phys.* **40**, 677 (1968); N. F. Mott and E. A. Davis, *Phil. Mag.* **17**, 1269 (1968); N. F. Mott and W. D. Twose, *Advan. Phys.* **10**, 107 (1961); N. F. Mott, *Can. J. Phys.* **34**, 1356 (1956).
- ³⁴C. T. Elliott, John Melngailis, T. C. Harman, and J. A. Kafalas, *Bull. Am. Phys. Soc.* **16**, 401 (1971).
- ³⁵R. Kubo, S. J. Miyake, and N. Hashitsume, in *Solid State Physics*, edited by F. Seitz and D. Turnbull (Academic, New York, 1965), Vol. 17, p. 361.
- ³⁶N. B. Brandt, Y. A. Svistova, Yu. G. Kashirskiy, and L. V. Lyn'kov, *Zh. Eksperim. i Teor. Fiz.* **56**, 65 (1969) [*Sov. Phys. JETP* **56**, 35 (1969)], and references therein.
- ³⁷E. H. Putley, in *Semiconductors and Semimetals*, edited by R. K. Willardson and A. C. Beer (Academic, New York, 1966), Vol. 1, p. 289.
- ³⁸H. Miyazawa, *J. Phys. Soc. Japan* **26**, 700 (1969).
- ³⁹G. Simmons and H. Wang, *Single Crystal Elastic Constants, A Handbook*, 2nd ed. (MIT Press, Cambridge, Mass., 1971).

Thermal Brillouin Scattering in Cadmium Sulfide: Velocity and Attenuation of Sound; Acoustoelectric Effects*

A. S. Pine

Lincoln Laboratory, Massachusetts Institute of Technology, Lexington, Massachusetts 02173

(Received 17 May 1971)

The velocity and attenuation of 35-GHz longitudinal *c*-axis acoustic phonons have been measured as a function of temperature and free-carrier concentration by high-resolution Brillouin spectroscopy. These measurements determine both the acoustoelectric and the anharmonic contributions to the phonon damping for comparison to theoretical models.

I. INTRODUCTION

The velocity and attenuation of 35-GHz longitudinal *c*-axis hypersonic waves have been measured as a function of temperature between 100 and 400 °K in both high- and low-conductivity cadmium sulfide. Data are obtained by high-resolution thermal Brillouin spectroscopy employing tandem interferometer analysis of the back-scattered 6328-Å light. The acoustoelectric and the anharmonic contributions to the Brillouin linewidth—hence the acoustic attenuation—are distinguished by their dependence on temperature and electron concentration. The anharmonic damping increases monotonically with temperature and is quite similar to

that observed previously in α -quartz,¹ which is an insulator. This phonon-phonon interaction is compared to a recent theory by Niklasson² from which it is found that a single-relaxation-time approximation for thermal phonons poorly represents the data. The acoustoelectric damping, manifest as a low-temperature peak, is examined with an acoustic frequency on the order of the dielectric-relaxation and diffusion frequencies. Also, since the acoustic wavelength here is on the order of the electron mean free path, generalization of the low-frequency Hutson-White³ acoustoelectric theory must be made. Diffusion effects play a significant role in this high-frequency study, so the results are sensitive to space-charge trapping. Furthermore

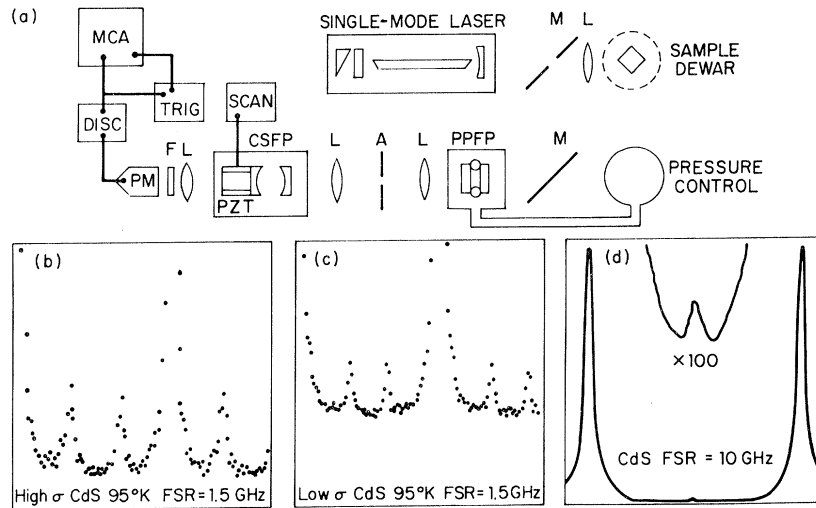


FIG. 1. Experimental high-resolution tandem Brillouin spectrometer and CdS spectra. (a) PFPF and CSFP: plane-parallel and confocal-spherical interferometers; MCA: multichannel analyzer; L: lens; M: mirror; A: aperture; F: filter; PM: photomultiplier (FW1so). (b), (c), and (d) are high- and low-resolution traces from CdS.

the data indicate some evidence for an energy-dependent relaxation-time approximation for the Boltzmann collision integral.

Brillouin scattering has been demonstrated by others⁴⁻⁶ to be an effective probe of the high-acoustic-flux domains generated by strong electric fields in piezoelectric semiconductors. Usually the small Brillouin shift was inferred from the small scattering angle, and the intensity and polarization properties of the scattered light gave information about the domain composition.^{4,6} In addition, Smith⁵ has been able to observe and spectrally analyze the thermal-phonon background with no applied field. The present experiment is a higher-resolution extension of these previous works, capable of giving detailed information about the acoustical interaction with the electrons and phonons in the crystal.

II. EXPERIMENTAL RESULTS

The high-resolution Brillouin spectrometer used to obtain the hypersonic velocity and attenuation in CdS is shown in Fig. 1(a). The signal-averaging and drift-compensating features of the apparatus have been discussed by Durand and Pine⁷ except for the interferometer prefilter necessitated by the strong unshifted light scattered from the defects and surfaces of the crystals. This low-resolution filter is a pressure-tuned plane-parallel Fabry-Perot (PFPF) interferometer with a free spectral range adjusted for overlap of the Brillouin-Stokes and anti-Stokes spectra, as seen in the trace of Fig. 1(d). With the filter tuned for this overlap, the accumulated data of the multiscanned high-resolution confocal spherical Fabry-Perot (CSFP) interferometer are shown in Figs. 1(b) and 1(c). These low-temperature spectra for high- and low-conductivity samples of CdS are displayed. The crystals are mounted on the cold finger of a double

Dewar with a thermocouple embedded in the mount. The high-conductivity sample ($\sigma_0 = 0.07$ mho/cm at 300 °K) is nominally pure $2 \times 2 \times 1$ -cm³ crystal grown by Harshaw. The low-conductivity sample ($\sigma_0 < 10^{-5}$ mho/cm at 300 °K in the dark) is a sulfur-compensated nominally pure $1 \times 1 \times 1$ -cm³ crystal grown by Crysteco. They are oriented for back scattering from longitudinal-acoustic waves propagating along with c axis within $\sim 2^\circ$. The single-mode He-Ne laser emits ~ 5 mW at 6328 \AA which is enough to give good counting statistics through the tandem interferometers with integration times of 10-60 sec.

The Brillouin shift ν_B and the linewidth $\delta\nu$ obtained from the two samples are plotted in Fig. 2 as a function of temperature. Here $\delta\nu$ is the full width at half-maximum of a Lorentzian line shape which, when convolved with the instrumental profile, fits the experimental width. The linewidth is proportional to the acoustic attenuation or damping, and the anharmonic and acoustoelectric contributions are additive. In the low-conductivity crystal the acoustoelectric effect is negligible, so the solid and dashed lines are the smoothed experimental division of the high-conductivity data into a phonon-phonon width $\delta\nu_p$ and an electron-phonon width $\delta\nu_e$. The Brillouin shifts in Fig. 2(a), from which the sound velocity is computed, are precise to within 0.1%. Therefore the difference in ν_B at low temperature for the high- and low- σ_0 crystals is outside of experimental error and probably results from the acoustoelectric-relaxation dispersion. These results are analyzed and compared with theory and other experiments in Secs. III-V.

III. VELOCITY OF SOUND

The Brillouin shift is related to the sound velocity $v(\vec{q})$ by

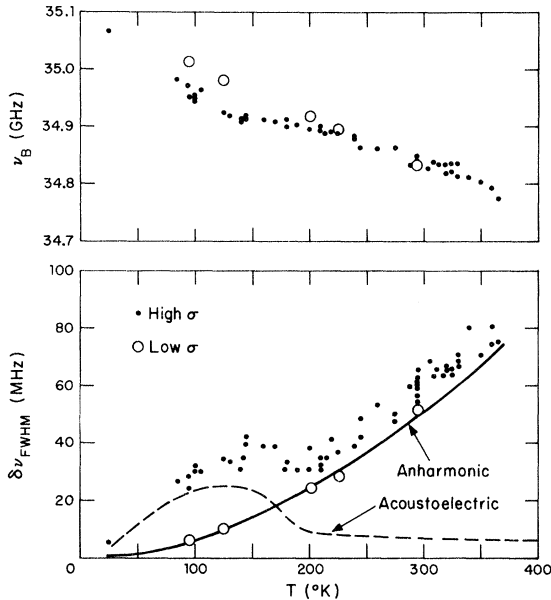


FIG. 2. Brillouin shift and linewidth from longitudinal-acoustic phonons along c axis in CdS.

$$\nu_B = [2nv(\vec{q})/\lambda_i] \sin \frac{1}{2} \theta, \quad (1)$$

where λ_i is the incident-light wavelength, n is the index of refraction at λ_i and temperature T , and θ is the scattering angle. In the back-scattering geometry, $\theta = 180^\circ$; so the phonon frequency $\omega = v(q)q = 2\pi\nu_B$ is maximized and the frequency spread $\delta\nu_\theta$ due to a finite acceptance angle $\delta\theta$ is minimized.⁷ This small spread of 1.3 MHz for CdS is due to the explicit angular dependence in (1) and the anisotropy in $v(\vec{q})$; the correction has been applied to the data in Fig. 2(b).

The velocity of the c -axis longitudinal-acoustic phonon is plotted from the Brillouin shift in Fig. 3 along with lower-frequency determinations. The refractive index at 295 °K is taken from the prism measurement of Bieniewski and Czyzak⁸ and its temperature dependence from the fringe counting method of Langer.⁹ The discrepancies among the various velocity measurements at 295 °K are about the maximum expected dispersion ($\sim 1.2\%$) due to the variable electron screening of the piezoelectric stiffening. The theory of this dispersion is reviewed later; it results in higher velocity for higher frequency or lower conductivity. However, the low-temperature velocity discrepancy between the Brillouin data and Gerlich's¹⁰ ultrasonic measurements is much too large to resolve in this way and is far outside experimental error. The refractive-index data of Langer⁹ are most suspect in this regard since his slope $\partial n/\partial T$ at 295 °K is a factor of 3 greater than that of Thomas and Sopori¹¹ who used the same technique for $T \geq 295$ °K; a final

determination of the temperature dependence awaits more definitive $n(T)$ data. Also, it is felt that this discrepancy is not caused by a sample dependence or misorientation since several crystals were found to be within the limits of Fig. 2(a) and the velocity anisotropy is small.^{10,12}

IV. ANHARMONIC DAMPING

Acoustic attenuation from phonon-phonon collisions occurs from two distinct processes. First, the acoustic wave may decay into two lower-frequency phonons, and second it may scatter a higher-frequency phonon. The first decay scheme is very wave-vector dependent and is generally negligible compared to the scattering process for acoustic wave vector q , much less than the zone-edge wave vector Q_{\max} . The scattering process, on the other hand, can explain the order of magnitude of the anharmonic damping and has been the subject of many theoretical models.^{2,13-18} The recent Green's-function theory by Niklasson² is the most general of these in that it is appropriate for the widest range of experimental conditions and in that the preceding models may all be derived from it as limiting cases.

With the assumptions of harmonic and anharmonic isotropy and a single relaxation time for thermal phonons dominated by umklapp rather than normal processes, Niklasson gives for the phonon-phonon linewidth or attenuation,

$$\frac{\delta\nu_p}{2\nu} = \frac{\alpha_p v(q)}{\omega} = -\frac{\gamma^2 C_v T}{4\rho v^2(q)} \text{Im} \left(I(\omega) + \frac{iI^2(\omega)}{2\omega\tau_p - iI(\omega)} \right), \quad (2a)$$

$$I(\omega) = \sum_j \int_0^{Q_{\max}} dQ Q^2 \Omega_j^2(Q) n_j(Q) [1 + n_j(Q)] G(Q, \omega) /$$

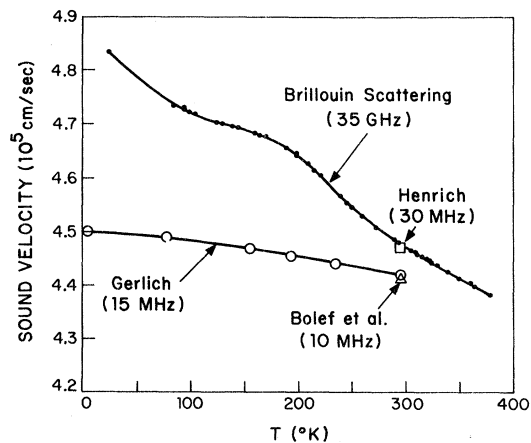


FIG. 3. Velocity of longitudinal-acoustic phonons along c axis in CdS from Brillouin scattering and ultrasonics measurements.

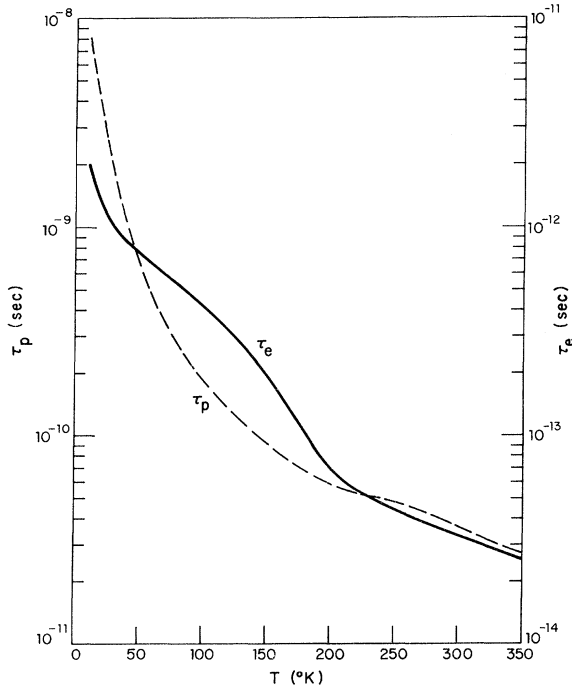


FIG. 4. Electron and thermal-phonon relaxation times in CdS.

$$\frac{2\pi^2 C_v k T^2}{\hbar^2}, \quad (2b)$$

$$G(Q, \omega) = \frac{1}{\beta_j(Q)} \ln \left(\frac{1 - i\omega\tau_p[1 + \beta_j(Q)]}{1 - i\omega\tau_p[1 - \beta_j(Q)]} \right), \quad (2c)$$

$$\beta_j(Q) = \left(\frac{\partial \Omega_j(Q)}{\partial Q} \right) / v(q), \quad (2d)$$

$$n_j(Q) = (e^{\hbar \Omega_j(Q) / k T} - 1)^{-1}. \quad (2e)$$

Here the thermal phonons of wave vector Q have frequencies $\Omega_j(Q)$ for branch j , boson occupation

factors $n_j(Q)$, group velocities $\partial \Omega_j / \partial Q$, and uniform relaxation time τ_p . C_v is the heat capacity at constant volume, ρ is the density, and γ is the averaged dimensionless Grüneisen parameter of order unity which scales the anharmonicity. The formal theory of Niklasson does not require the approximations of isotropy and a lifetime independent of $\Omega_j(Q)$. However, the theory is more tractable in this form and contact can be made with independently measured parameters. It is of interest to see if these assumptions are too restrictive to explain the Brillouin data.

The thermal-phonon relaxation time is calculated from the thermal conductivity κ in CdS measured by Holland¹⁹ according to

$$\kappa = \frac{1}{3} C_v \bar{v}^2 \tau_p \quad (3)$$

and is plotted in Fig. 4. Here the velocity \bar{v} is a Debye average of the longitudinal- and transverse-acoustic velocities given by

$$\bar{v} = \left(\frac{1}{3} v_l^{-3} + \frac{2}{3} v_t^{-3} \right)^{-1/3} \approx 2 \times 10^5 \text{ cm/sec for CdS}. \quad (4)$$

The heat capacity is computed from the Debye model with a Debye temperature of 200 °K as obtained from a lattice-dynamics calculation for CdS by Goel and Singh.²⁰

The anharmonic model of Woodruff and Ehrenreich¹⁴ is derived from Eq. (2) in the dispersionless case for which $\Omega_j(Q) = vQ$, $\beta_j(Q) = 1$, and

$$I(\omega) = G(Q, \omega) = \ln(1 - 2i\omega\tau_p).$$

The damping predicted by this theoretical model is present in Fig. 5 for comparison with the experimental anharmonic linewidth. Here the normalization $\gamma^2 = 2.3$ is taken to fit the high-temperature data. A similar calculation for thermal phonons with a model dispersion

$$\Omega_j(Q) = (2/\pi)v(q)Q_{\max} \sin(\pi Q/2Q_{\max})$$

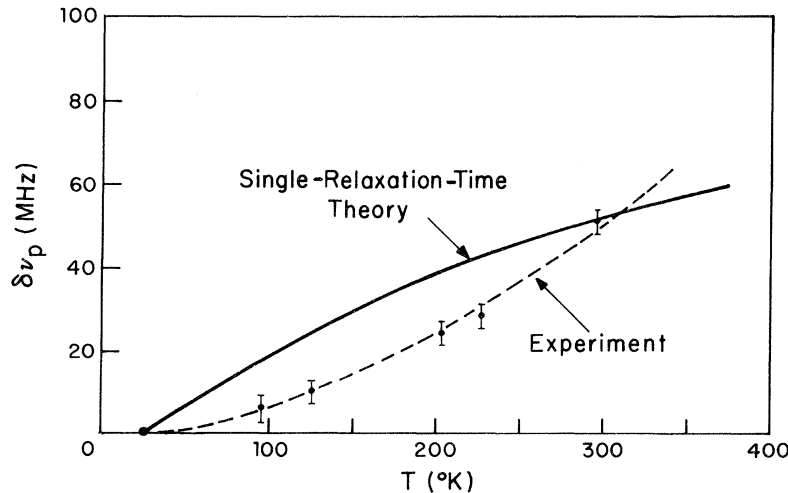


FIG. 5. Experimental and theoretical anharmonic damping in CdS.

is virtually indistinguishable from the Woodruff-Ehrenreich theory for the temperatures of interest. An Einstein model for the thermal phonons, Ω_j independent of Q , proposed by Bömmel and Dransfeld¹³ diverges significantly from the plotted theory only for $T < 100$ °K.

It is seen in Fig. 5 that the trend of the single-relaxation-time theory does not well represent the data. The reason for this is apparent from the Woodruff-Ehrenreich model noting that $\omega\tau_p > 5$ for the temperatures of this experiment. For $\omega\tau_p \gg 1$, the temperature dependence of the damping is dominated by the $C_v T$ factor of (2a) which is roughly the shape of the theory in Fig. 5. Shorter lifetimes only enhance this curvature giving a worse fit to the data. This same conclusion was reached in an earlier study of the anharmonic linewidth in α -quartz.¹ There it was shown that the shape of the curve could be improved by using a distributed relaxation time in a theory due to Kwok.¹⁷ The Kwok theory is equivalent to the Niklasson expression (2a) if the second term in the brackets is omitted and τ_p is taken to depend on Q . This second term arises from so-called vertex² or local-temperature correlations and becomes negligible for large $\omega\tau_p$. In the quartz work the model for $\tau_p(Q)$ was taken to be anharmonic decay of the thermal phonon into two lower-frequency modes. This model also can be fit to the CdS data, but it is not given since no independent measure of $\tau_p(Q)$ exists.

V. ACOUSTOELECTRIC DAMPING

Acoustic attenuation by electron-phonon collisions in piezoelectric semiconductors was first considered by Hutson and White.³ Their classical approach with a local relation between currents and fields was implicitly restricted to $ql \ll 1$. Here q is the phonon wave vector and l is the electron mean free path. Several workers²¹⁻²³ have used a Boltzmann-equation formulation to generalize the theory for all ql . The resultant theory with no external fields is

$$\frac{\delta\nu_e}{2\nu} = \frac{\alpha_e v(q)}{\omega} = -(K_{pe}^2 + K_{dp}^2) \text{Im}H, \quad (5a)$$

$$\frac{v(q) - v(0)}{v(0)} = -K_{dp}^2 + (K_{pe}^2 + K_{dp}^2) \text{Re}H, \quad (5b)$$

$$H = \frac{1 + if\omega/\omega_D}{1 + i(\omega_c/\omega + f\omega/\omega_D)}. \quad (5c)$$

Here the electromechanical coupling constants for piezoelectric and deformation-potential interactions are given by

$$K_{pe}^2 = d_{33}^2/2\epsilon_3 c_{33}, \quad (6a)$$

$$K_{dp}^2 = \epsilon_3 q^2 \chi^2/2e^2 c_{33}. \quad (6b)$$

The piezoelectric constant d_{33} , the dielectric con-

stant ϵ_3 , and the elastic constant c_{33} are pertinent to the c -axis longitudinal-acoustic phonon. For CdS,²⁴ $K_{pe}^2 = 0.012$, and for a reasonable deformation potential $\chi = 10$ eV, $K_{dp}^2 \sim 10^{-2} K_{pe}^2$; so the piezoelectric coupling dominates. The dielectric-relaxation frequency ω_c and the diffusion frequency ω_D are given in terms of the frequency- and wave-vector-dependent conductivity:

$$\omega_c = \sigma(q, \omega)/\epsilon_3, \quad (7a)$$

$$\omega_D = v^2(q)/R(q, \omega), \quad (7b)$$

$$R(q, \omega) = \frac{kT\sigma(q, \omega)}{n_e e^2 (1 - i\omega\tau_e)}. \quad (7c)$$

Here n_e is the free-electron concentration and τ_e is the electron lifetime obtained from the mobility data of Devlin²⁵ and plotted in Fig. 4. The dc conductivity, mobility, and lifetime are related by

$$\sigma_0 = n_e e \mu = n_e e^2 \tau_e / m^*. \quad (7d)$$

The effective mass $m^* \approx 0.2m$ for CdS.²⁵ The electron mean free path for nondegenerate statistics is given by

$$l = \tau_e (2kT/m^*)^{1/2}. \quad (7e)$$

The high-conductivity sample has a carrier concentration $n_e = 1.2 \times 10^{15} \text{ cm}^{-3}$. Defining a dimensionless parameter

$$x = (1 - i\omega\tau_e)/ql, \quad (8a)$$

the generalized conductivity may be written

$$\sigma(q, \omega) = \sigma_0 (2x/ql) [1 - \pi^{1/2} x F(x)], \quad (8b)$$

where $F(x)$ is related to the plasma-dispersion function,²⁶

$$F(x) = \frac{2}{\pi^{1/2}} e^{x^2} \int_x^\infty e^{-t^2} dt. \quad (8c)$$

The theory for the attenuation and velocity dispersion, (5), is now completely defined except for the parameter f which is the untrapped fraction of the space charge.³ As mentioned in connection with the velocity measurements, the maximum dispersion, as seen in (5b), for high frequency or low conductivity is $[v(\infty) - v(0)]/v(0) = K_{pe}^2$.

In this Brillouin experiment, $ql \sim 1$, so the generalized conductivity must be used. The Hutson-White theory is derived by setting $ql \rightarrow 0$, where $\sigma(q, \omega) \rightarrow \sigma_0$. The generalized theory (5)–(8) is compared to the Hutson-White limit in Fig. 6 for 35-GHz phonons in the extreme cases of complete ($f=0$) and no ($f=1$) trapping. The Hutson-White limit is at variance with the generalized theory chiefly at low temperatures where $ql \gtrsim 1$. The phonon frequency in this study is higher than the diffusion frequency, in contrast to most earlier ultrasonics experiments in CdS. The diffusion effects, which are turned on theoretically by setting

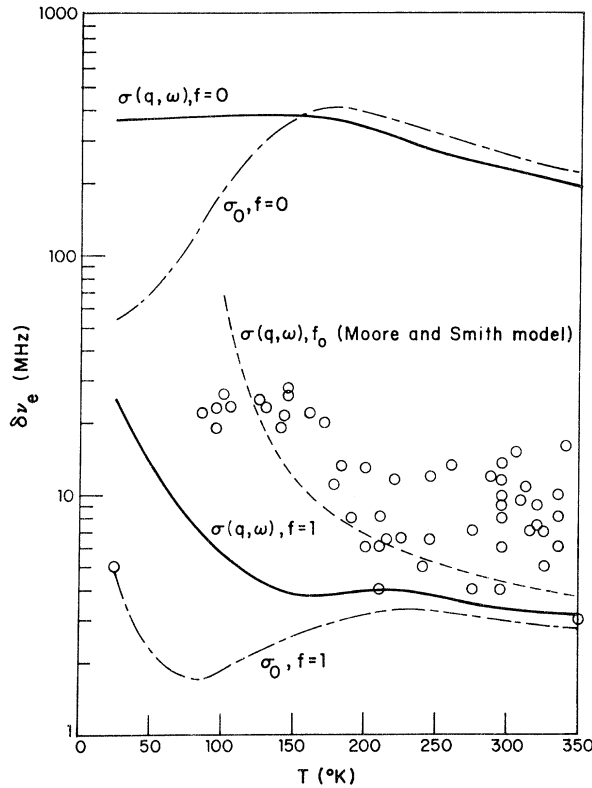


FIG. 6. Experimental and theoretical acoustoelectric damping in *n*-type CdS for $\nu = 35$ GHz and $n_e = 1.2 \times 10^{15}$ cm $^{-3}$: The smoothed anharmonic-damping contribution has been subtracted from the data; typical precision is ± 5 MHz, giving rise to the large data scatter above 200 °K on the log plot. Hutson-White theory indicated by σ_0 , generalized theory by $\sigma(q, \omega)$; mobile space charge fraction by f , Moore-Smith frequency-independent f model by f_0 (see text).

$f=1$ since they enter via the factor $f\omega/\omega_D$, reduce the attenuation (or the gain in an acoustoelectric amplifier) by nearly two orders of magnitude. This is an important consideration when designing acoustoelectric devices at high frequencies.

Clearly the theoretical model is a sensitive function of f ; and since most of the data fall between $f=0$ and 1, a trapping model could be devised to fit the data. In general, f may be a complex frequency- and temperature-dependent function. Moore and Smith²⁷ have measured f in high-conductivity CdS (semiconducting Eagle-Picher UHF crystal) by a current-saturation technique. Their experimental data above 77 °K are explained by a single-trap-level model given by

$$f_0 = [1 + (N_t/N_e) e^{E_t/kT}]^{-1} . \quad (9)$$

Here $N_t = 1.3 \times 10^{17}$ cm $^{-3}$ is the trap concentration, $E_t = 0.017$ eV is the trap activation energy, and

$N_e = 4.2 \times 10^{14} T^{3/2}$ is the conduction-band density of states. Ignoring for the moment the frequency dependence of f and inserting f_0 for f in (5), the dashed curve of Fig. 6 results. This model accounts for the trend of the data above 100 °K, but the difference in samples may cause the disagreement in detail. At lower temperatures, carrier freezeout may give rise to the observed drop in acoustoelectric damping—even below the $f=1$ curve where the 25 °K datum is found. Direct conductivity measurements made on the Harshaw crystal track Devlin's²⁵ mobility down to 80 °K implying no freezeout; however, at 25 °K the indium contacts (ultrasonically bonded) cracked loose and no electrical measurements could be made. Moore and Smith²⁷ did obtain evidence of carrier freezeout at low temperatures in their semiconducting sample.

The frequency dependence of f , arising from finite trapping times, has been discussed by several authors.^{24,27-29} Trapping times measured by Moore and Smith²⁷ in CdS are too slow to follow the Brillouin frequency at any temperature of this experiment. Thus there should be little effective trapping and the data should be compared to the $f=1$ limit in Fig. 6. The discrepancy here is significant and may be due to the single-relaxation-time assumption for the Boltzmann collision integral used in (5)–(8). Jacoboni and Prohofsky³⁰ have extended the theory of acoustoelectric absorption by using energy-dependent relaxation times. They find an enhancement of the absorption at high frequencies for a model calculation appropriate to ionized impurity scattering in GaAs at 77 °K. This is in qualitative agreement with these results on CdS. However, only the average-mobility lifetime has been measured, so it is difficult to confirm any distributed τ_e model for application to this experiment.

In summary then for both the anharmonic and the acoustoelectric damping, single-relaxation-time theories are capable of explaining the magnitude, but not the detailed shape, of the experimental attenuation with no adjustable parameters. More realistic theories exist but the parameters are not easily measured. The relatively poor fit of the simple models to the high-frequency Brillouin data is something of a surprise because of the success of these models for lower-frequency results.

ACKNOWLEDGMENTS

The author would like to thank V. E. Henrich and D. L. Spears for several helpful discussions on the acoustoelectric effect. The author is further indebted to K. W. Nill on this same subject for clarification of the generalized conductivity and for his computer program to calculate it.

*This work was sponsored by the Department of the Air Force.

¹A. S. Pine, in *Light Scattering Spectra of Solids*, edited by G. B. Wright (Springer-Verlag, New York, 1969), p. 581.

²G. Niklasson, *Ann. Phys. (N. Y.)* **59**, 263 (1970).

³A. R. Hutson and D. L. White, *J. Appl. Phys.* **33**, 40 (1962).

⁴J. Zucker and S. Zemon, *J. Acoust. Soc. Am.* **49**, 1037 (1970), and references therein.

⁵R. W. Smith, *J. Acoust. Soc. Am.* **49**, 1033 (1971), and references therein.

⁶D. L. Spears, *Phys. Rev. B* **2**, 1931 (1970), and references therein.

⁷G. E. Durand and A. S. Pine, *IEEE J. Quantum Electron.* **4**, 523 (1968).

⁸T. M. Bieniewski and S. J. Czyzak, *J. Opt. Soc. Am.* **53**, 496 (1962).

⁹D. W. Langer, *J. Appl. Phys.* **37**, 3530 (1966).

¹⁰D. Gerlich, *J. Phys. Chem. Solids* **28**, 2575 (1967).

¹¹G. Thomas and B. L. Sopori, *J. Appl. Phys.* **41**, 603 (1970).

¹²D. I. Bolef, N. T. Melamed, and M. Menes, *J. Phys. Chem. Solids* **17**, 143 (1960).

¹³H. E. Bömmel and K. Dransfeld, *Phys. Rev.* **117**, 1245 (1960).

¹⁴T. O. Woodruff and H. Ehrenreich, *Phys. Rev.* **123**, 1553 (1961).

¹⁵H. J. Maris, *Phil. Mag.* **9**, 901 (1964).

¹⁶S. Simons, *Proc. Phys. Soc. (London)* **83**, 749 (1964).

¹⁷P. C. Kwok, Ph.D. thesis (Harvard University, 1965) (unpublished).

¹⁸R. Klein, *Physik Kondensierten Materie* **6**, 38 (1967).

¹⁹M. G. Holland, *Phys. Rev.* **134**, A471 (1964).

²⁰N. S. Goel and R. P. Singh, *Indian J. Pure Appl. Phys.* **1**, 343 (1963).

²¹H. N. Spector, in *Solid State Physics*, edited by F. Seitz and D. Turnbull (Academic, New York, 1966), Vol. 19, p. 291, and references therein.

²²K. W. Nill, Ph.D. thesis (MIT, 1966) (unpublished).

²³C. Jacoboni and E. W. Prohofsky, *J. Appl. Phys.* **40**, 454 (1969).

²⁴V. E. Henrich and G. Weinreich, *Phys. Rev.* **178**, 1204 (1969).

²⁵S. S. Devlin, in *Physics and Chemistry of II-VI Compounds*, edited by M. Aven and J. S. Prener (Wiley, New York, 1967), p. 549.

²⁶B. D. Fried and S. D. Conte, *The Plasma Dispersion Function* (Academic, New York, 1961).

²⁷A. R. Moore and R. W. Smith, *Phys. Rev.* **138**, A1250 (1965).

²⁸C. A. A. J. Greebe, *Phys. Letters* **4**, 45 (1963).

²⁹I. Uchida, T. Ishiguro, Y. Sasaki, and T. Suzuki, *J. Phys. Soc. Japan* **19**, 674 (1964).

³⁰C. Jacoboni and E. W. Prohofsky, *Phys. Rev. B* **1**, 697 (1970).

Resonance Brillouin Scattering in Cadmium Sulfide[†]

A. S. Pine

Lincoln Laboratory, Massachusetts Institute of Technology, Lexington, Massachusetts 02173

(Received 17 May 1971)

A weak resonant enhancement of the Brillouin-scattering cross section is observed as the fundamental absorption edge of cadmium sulfide is thermally tuned through the incident radiation at 5145 Å. The data are compared to light-scattering theory where the parameters are determined by optical absorption. In regions of high absorption, the spectral width of the Brillouin scattering is increased due to the optical wave-vector spread; this provides an independent measurement of the absorption.

I. INTRODUCTION

A weak resonant enhancement of the Brillouin-scattering cross section is observed as the fundamental absorption edge of cadmium sulfide is thermally tuned through the incident radiation at 5145 Å. This study complements earlier measurements by Tell, Worlock, and Martin¹ of the enhancement of the Pockel's electro-optic coefficients in CdS and ZnO. Here by back scattering from thermal phonons, the highly absorbing band-gap region can be approached more closely than with the low-acoustic-frequency small-angle-scattering technique used by Tell *et al.*¹ The resonant behavior for scattering from longitudinal acoustic (LA) waves propagating along either the *c* or *a*

axis is essentially the same. This implies that the electro-optic contribution to the scattering from the piezoelectric field associated with the *c*-axis LA phonon² does not dominate the resonance effects the way that the polar fields associated with the LO phonons do in Raman scattering. When the measured Brillouin count rate is suitably corrected for the varying temperature and scattering volume, the cross section is found to increase roughly as the square root of the absorption. Between 100 and 300 °K the absorption increases by over three orders of magnitude. This resonance enhancement is characterized as weak since it is less than one would predict by Loudon's³ theory assuming that the electron-hole-pair states responsible for the absorption are the intermediate virtual states of